https://doi.org/10.1016/j.jece.2020.104491

Removing arsenate from water using modified manganese oxide ore: column adsorption and waste management

Thi Thuc Quyen Nguyen, Paripurnanda Loganathan, Tien Vinh Nguyen*, Saravanamuthu Vigneswaran

Faculty of Engineering and IT, University of Technology Sydney, 15 Broadway, Ultimo, NSW, 2007, Australia

* Corresponding author: Tien Vinh Nguyen, Email: Tien.Nguyen@uts.edu.au; Tel: 61-2-95142620; Fax: 61-2-95147803

The bed volumes of water (As concentration 0.1 mg/L) treated to maintain the As(V) concentration below the WHO guideline concentration (C_{WHO} = 10 µg/L) were 8 and 16 times higher for Fe^a-VMO; 6 and 12 times higher for Zr^a-VMO, than for unmodified VMO at flow velocities of 0.15 and 0.5 L/h, respectively.

Abstract

There is a need to remove arsenic (As) in drinking water supplies by simple and cost-effective techniques. A column adsorption study was conducted to remove As(V) from water employing a Fe and Zr grafted Vietnam manganese oxide ore (Fe^a-VMO and Zr^a-VMO). At flow rate of 0.15 L/h, the bed volumes of water (As(V) concentration 0.1 mg/L) treated by Zr^a-VMO and Fe^a-VMO to produce water with As(V) concentration below the WHO guideline concentration (10 µg/L) were 6 and 8 times higher than for VMO, respectively. When the flow rate increased to 0.5 L/h, the corresponding bed volumes for Zr^a-VMO and Fe^a-VMO were 12 and 16 times higher than for unmodified VMO. An increase in influent As concentration increased the adsorption capacity, but the increase of flow rate reduced the adsorption capacity. The maximum adsorption capacities derived from the Thomas model for VMO, Fe^a-VMO, and Zr^a-VMO at an influent concentration of 0.25 mg As(V)/L, and flow rate of 0.15 L/h were 0.151, 1.145, and 0.925 mg/g, respectively. These values fell when influent As concentration decreased or the flow rate increased. Solidification/stabilisation method was applied to immobilise As(V) in the exhausted absorbent wastes by replacing 5, 10, 15, and 20% of sand in a sand/cement concrete mixture by the adsorbent waste. This solidified material had satisfactory compressive strength, rapid chloride penetrability test, and volume of permeable voids, which indicated the material had good stability, making it suitable for use as a building material in construction work. The As(V) leaching from these materials, as measured by Method 1313 of the Leaching Environmental Assessment Framework of USEPA, proved to be very negligible.

Keywords: *Arsenate removal; adsorption; modified manganese oxide ore; solid waste management; solidification/stabilisation*

1 Introduction

Inorganic arsenic (As) is acknowledged as one of the most serious toxic pollutants in drinking water. Elevated concentrations of As have been reported in groundwater in many parts of the world, especially in developing countries such as Bangladesh, India, Nepal, Cambodia, Vietnam, etc., where groundwater is used as the primary drinking water source in rural areas [1]. Historically, various technologies have been applied to remove As contamination in water, such as oxidization, precipitation, coagulation, adsorption, ion-exchange, and use of membranes. Each method has advantages and disadvantages. Of these processes, adsorption is the most cost-effective, simple, and efficient one as it can even remove tiny amounts of As from water, and therefore, it has been widely used [2]. Moreover, it produces minimum chemical or biological sludge waste and the adsorbent can be restored and used repeatedly, thus curtailing the operation costs [3]. A large number of natural and synthetic materials, have been used as adsorbents for As removal. Some commercial and synthetic media, for example activated carbon, activated alumina and Zr resin were reported to have a very high As adsorption capacity (more than 10 mg/g [4]). On the other hand, several natural materials or waste industrial/agricultural products (including sand, natural clay, kaolinite clay, bentonite, laterites, manganese ore, iron ore, dry plants, red mud, fly ash, etc.) have surfaced as low-cost As removal alternatives [5–7]. Unlike commercial products, some natural materials cannot reach As adsorption capacity higher than 1 mg/g. In some cases, they could not even meet the As permissible limit for practical application [8]. However, when compared to the most popular and efficient As adsorbent, such as activated carbon which has a high price and regeneration cost, the natural materials' advantages are cost-effectiveness, mechanical stability and local availability in many As affected areas [7]. This has promoted the use of low-cost locally available natural adsorbing materials that are affordable and simple to use by inhabitants in low-income regions, where most As pollution exists [9].

Our previous study found that arsenate (As(V)) could be removed effectively by the adsorption process using a low-cost natural manganese oxide ore (VMO) and its modified forms [1]. The Langmuir maximum As adsorption capacity of VMO, iron-modified VMO (Fe^a-VMO) and zirconium modified VMO (Zr^a-VMO) was identified as 0.11 mg/g, 2.19 mg/g and 1.94 mg/g (at an initial As(V) concentration of 0.5 mg/L), respectively. Based on the promising results obtained in static batch studies, these adsorbents were used in a column study for removing As(V)

from synthetic contaminated water under various conditions in the first part of the current study. The column study is more relevant to practical conditions in water treatment plants than the batch type.

After the adsorption treatment process, the exhausted adsorbent media must be well managed to prevent As being released into the environment. Four options could be chosen to treat the exhausted adsorbent waste, which includes: (1) desorption/regeneration (D/R), (2) concentration and containment, (3) dilution and dispersion, and (4) encapsulation of the material [4,10,11]. These options have been applied selectively depending on such issues as economic efficiency, safety, concentration, and purity of the substance. Practically, the D/R process is usually applied to valuable adsorbents and adsorbates. Because there is a limited demand for As in the market and it is unsafe to store the As after recovery, the D/R method used for valuable elements is not attractive for As [4]. Furthermore, the D/R approach has problems regarding: firstly, the safe disposal of the highly concentrated As in the desorbed solution; secondly, inability to completely desorb all the adsorbed As from the adsorbent; and thirdly, the decline in As adsorption capacity of the adsorbent after each adsorption cycle. The second method of concentration and containment is relatively costly and not affordable for local people, where most of the As-related problems exist. The third method of dilution and dispersion, although it reduces the immediate environmental problem of As, can cause environmental problems in the future at the site where it is repeatedly disposed. Moreover, humans exposed to low concentrations of As over the long-term will pose serious health problems [10].

Unlike other methods, the encapsulation option through solidification/stabilisation (S/S) is more attractive and considered to be an effective technique to treat As-containing solid waste [12]. The U.S. Environmental Protection Agency (USEPA) also recognized S/S processes as the Best Demonstrated Available Technology (BDAT) for the land disposal of hazardous elements [13]. The advantage of this method is that the toxic substance (As) is immobilised and incorporated into solid materials such as cement, slag or polymer so that the As-encapsulated materials become a reduced or non-hazardous solid waste [4,10]. Moreover, the S/S method can be cost-effective if the incorporation and stabilisation are done using a material that is manufactured locally for another purpose without affecting its quality. The product of the S/S process can be safely disposed of in a secure landfill or used as a construction material that has limited contact with humans.

The popular agents of the As(V) S/S process that have been evaluated successfully are cement and mixtures of cement, such as Portland cement, mixtures of Portland cement with iron (II, III), lime, fly ash, or silicate [4,10,14]. The advantages of these agents are that they are low-cost, easy to incorporate with wet/solid waste, and have high alkalinity, which could restrict the solubility of hazardous metals [15]. However, the As which is incorporated and stabilised into

these materials should not leak out into the environment in the future. Some studies find that As concentration in leachates from the encapsulated materials determined according to the toxicity characteristic leaching procedure (TCLP) of USEPA was below the acceptable limit of 5 mg/L (below this concentration, As is unlikely to cause toxicity) [12,16]. However, detailed studies about the characteristics of encapsulated material regarding the physico-chemical characteristics with reference to the reaction of As within the encapsulated material and the potential As release in the long-term are limited. Moreover, evaluating the quality of the S/S product using measurements such as compressive strength, rapid chloride penetrability test (RCPT), and volume of permeable voids (VPV), which are important features to decide whether the construction material can be used widely or not, has been rarely performed.

The aims of this research were to evaluate the feasibility of disposing of the exhausted adsorbent waste by encapsulating it into concrete made from cement and test whether As leaching from the material is within the safety level. The physico-chemical characteristics of the encapsulated product and the possible reactions of As within the product are also investigated in this study to determine the product's stability.

2 Material and methods

2.1. Materials

A synthetic stock solution was prepared by dissolving 41.65 mg sodium arsenate ($Na_2HAsO_4 \cdot 7H_2O$) in 1 L Milli-Q water to obtain a concentration of 10 mg As(V)/L. Feed solutions with As(V) concentrations of 0.10 and 0.25 mg/L were prepared by spiking tap water with the stock solution. The solution pH was maintained at 7.0 ± 0.1 by adding nitric acid (0.1 M HNO_3) or sodium hydroxide (0.1 M NaOH).

A commercial Vietnamese manganese oxide (VMO), which is a mineral waste originating from the Tuyen Quang mine, and supplied by Phuong Nam Import-Export Trading and Service Joint Stock Company, Ha Noi, Vietnam, served as an adsorbent for As [1]. It is a low-cost material and employed locally as an adsorbent in water treatment systems. A$0.40/kg.

VMO for the study was produced by crushing and sieving the original manganese ore (0.3 - 3 mm) into a particle size of 0.3 - 0.6 mm. It was then modified using ferric nitrate nonahydrate ($Fe(NO_3)_3 \cdot 9H_2O$) and zirconyl chloride octahydrate ($ZrOCl_2.8H_2O$) to produce Fe grafted VMO (Fe^a-VMO) and Zr grafted VMO (Zr^a-VMO), respectively. The modification procedure has been described in detail elsewhere [1].

2.2 Column studies

Column adsorption studies were conducted using nine glass columns with a height of 50 cm. They were packed with 40 g of adsorbent (corresponding to 30 cm bed-height). 1.0 mm acrylic beads and cotton balls were used at the top and bottom of the column to prevent the release of adsorbent from the column. A dosing pump (Master flex L/S) was used to continuously pump the As solution through the columns in an up-flow mode at constant flow rates of 0.15 and 0.50 L/h (1.9 and 6.4 m/h). Samples were collected every 2 h on the first day and then once daily and weekly until the adsorbents were saturated with As. The pH of the effluent samples was nearly the same as the influent solution (pH 7.0 ± 0.2).

The samples were filtered using 0.45 µm filters and filtrates were analysed for As using an ICP-MS instrument (Agilent Technologies 7900 ICP-MS).

The total amount of As(V) adsorption, q_{total} (mg), and column experimental adsorption capacity, $q_{e,exp}$ (mg/g) were calculated manually from the breakthrough curves using Microsoft Excel spreadsheet according to the following equations [17,18]:

$$q_{total} = Q.\int_{t=0}^{t=total}(C_o - C_t)dt \quad [1]$$

$$q_{e,exp} = \frac{q_{total}}{m} \quad [2]$$

where Q is the volumetric flow rate (L/h), t is flow time (h), C_o is As(V) initial concentration (influent) (mg/L), C_t is As(V) concentration (effluent) at time t (mg/L), m is amount of adsorbent in the column (g).

The nonlinear Thomas model [19] was applied to describe the experimental data (equation 3):

$$\frac{C_t}{C_o} = \frac{1}{1+\exp\left(\frac{K_{Th}q_T m}{Q} - K_{Th}C_o t\right)} \quad [3]$$

where K_{Th} is the Thomas rate constant (L/h/mg), and q_T is the Thomas model adsorption capacity (mg/g).

2.3 Solidification/stabilisation

2.3.1 Concrete casting

The used exhausted adsorbents from the column experiments were rinsed quickly with tap water to remove the adsorbent residues stuck to the column surface. They were then dried at a temperature of 50 ^oC for 8 h. The As ions in the adsorbents would not have leached out of the adsorbents during the rinsing with water because they were strongly adsorbed through electrostatic adsorption forces and chemical bonds. The exhausted VMO, Fe^a-VMO and Zr^a-VMO adsorbents were mixed at a ratio of 1:1:1 and encapsulated with concrete. Five levels of the exhausted

adsorbents were used in the concrete mix. The compositions of the 5 mixtures are shown in Table 1. The concrete mix samples are named C0, C5, C10, C15, C20, corresponding to the replacement levels of sand by the exhausted adsorbent mixture (0%, 5%, 10%, 15%, and 20%). The materials for the concrete mix, such as river sand, aggregates (gravels of 10 - 20 mm size), and Portland cement, were supplied by a local construction material store. The concrete samples were prepared utilising a 100 mm x 200 mm cylindrical mould. One day after casting, the concrete samples were unmoulded and soaked in a curing chamber containing a lime solution for 27 days as described by Baweja et al. [20]. The weight of each fresh concrete sample was kept constant at 2365 kg per m^3. The initial As(V) loading was estimated based on the results of the column study and the proportions of the constituents in the concrete (Table 1). It is approximately 8.97, 17.95, 26.92, and 35.89 mg As(V) per 1 kg of fresh concrete corresponding to C5, C10, C15, and C20.

The characteristics of the final products were determined, and they consisted of compressive strength, RCPT, and VPV. Compressive strength was measured using UTC-4727G-2000 kN Capacity general purpose compression testing frame - standard method ASTM C39/C39M-20 [21]. In this method, a load of 0.25 ± 0.05 MPa/s was applied at a rate of movement, corresponding to a stress rate on the cylindrical sample, until the load indicator presents a steady decrease of the load, and the concrete sample displays a definite fracture pattern. The RCPT was measured using Proove's It - Germany Instrument in accordance with standard method ASTM C1202-19 [22]. In this method, a 50 mm-thick slice of the concrete sample was introduced to a potential of 60 V with two ends of the slice immersed in sodium chloride solution and sodium hydroxide solution, respectively. After 6h, the total charge that passed through the sample was measured to obtain the sample's resistance to chloride ion penetration. The VPV of the product was measured according to the standard method ASTM C642-13 [23]. The VPV percentage of each concrete sample was calculated based on the decrease in mass of a 50 mm-thick slice sample after drying in oven at 110 ^{o}C for 24 h, followed by immersing in water for 48 h and boiling for 5 h.

Table 1. Concrete mixture compositions

Name	Exhausted adsorbent waste (kg/m^3)	Sand (kg/m^3)	Aggregate gravels (kg/m^3)		Cement (kg/m^3)	Water (L/m^3)
			10 mm	20 mm		
C0	0	745	460	655	325	180
C5	37	708	460	655	325	180
C10	75	671	460	655	325	180
C15	112	633	460	655	325	180
C20	149	596	460	655	325	180

2.3.2 Leaching test

The leaching test on all concrete samples was conducted to determine whether leaching of As into the natural environment would comply with the stipulated USEPA regulation. Method 1313 of the Leaching Environmental Assessment Framework (LEAF), which was conducted in a batch extraction procedure, assessed the leaching potential [24]. This is a short-term procedure (24, 48 or 72 h, depending on the sample's particle size) performed at a wide range of pH (from 2 to 13).

The waste incorporated concrete sample (28 days-old) was crushed into a size of approximately 5 mm using a jaw crusher. The crushed concrete was then washed by deionized (DI) water to remove the dust and dried at 50 ^{o}C for 8 h. 80 g of each dried crushed concrete sample was mixed with 800 mL of DI water (solid/solution ratio of 1:10) whose pH was adjusted to 2, 4, 5.5, 7, 8, 9, 10.5, 12 and 13 using 2N HNO_3 and 1N KOH. The mixture was placed inside a 1L vessel and shaken at 28 ± 2 rpm for 72 h in an orbital shaker. The suspensions were filtered through 0.45 µm filters, and As in the filtrates was analysed using an Agilent Technologies 7900 ICP-MS instrument. The pH of the filtrate was also measured.

2.4 Characteristics of material

The characteristics of VMO, modified VMOs and the exhausted adsorbent encapsulated concrete samples were evaluated using Scanning electron microscopy/energy-dispersive X-ray spectroscopy (SEM/EDS, Quanta-650 instrument), and X-ray diffraction (XRD, Empyrean-PANalytical instrument, Netherlands). These have been described in detail elsewhere [1].

3. Results and discussion

3.1 Characteristic of adsorbents

The characteristics of the original VMO and modified VMOs have been described in detail recently [1]. Briefly, the XRD analysis showed that VMO consists of minerals such as quartz, goethite, cryptomelane, and muscovite. The main chemical elements other than oxygen present in VMO are Mn (25.6%), Fe (16.1%), and Si (13%). The amount of Fe rose to 21.9% after Fe grafting (Fe^a-VMO), and the amount of Zr after Zr grafting was 9.8% (Zr^a-VMO) as determined by XRF measurement [1]. FTIR measurement identified that the chemical bonds present in these adsorbents are -O-H, -C-H, -Fe-OH, Fe-O, Si-O, Zr-O-Zr [1]. The zero points of charge of original VMO, Fe^a-VMO, and Zr^a-VMO are 6.3, 7.5, and 7.1, respectively, which reduced to 5.4, 7.1, and 6.8 after As(V) adsorption [1]. The reduction in the zero points of charge indicated that As(V) was mainly adsorbed by inner-sphere complexation, i.e. ligand exchange/chemical adsorption [3].

Fig. 1 presents the SEM images of the surface morphologies of the original VMO and modified VMOs. As described in the previous study, the modification at high temperature (550 ^oC) had changed the surface structure of the original VMO with more porous layers/channels. However, there is no visible change in the morphology of the adsorbents even if many days have passed after As(V) adsorption. Effluent samples from the columns had no detectable Fe or Zr, which indicates these metals in the modified VMO remained intact and well-conserved. Because original VMO contained many elements, mainly Mn, Fe, Al, these elements could leach out from VMO into the treated water. This was checked by analysing these elements in the leachates. The results showed that the Al concentration in the leachates was below the detection limit, while Fe and Mn concentrations were very low (0.002 and 0.001 mg/L, respectively)

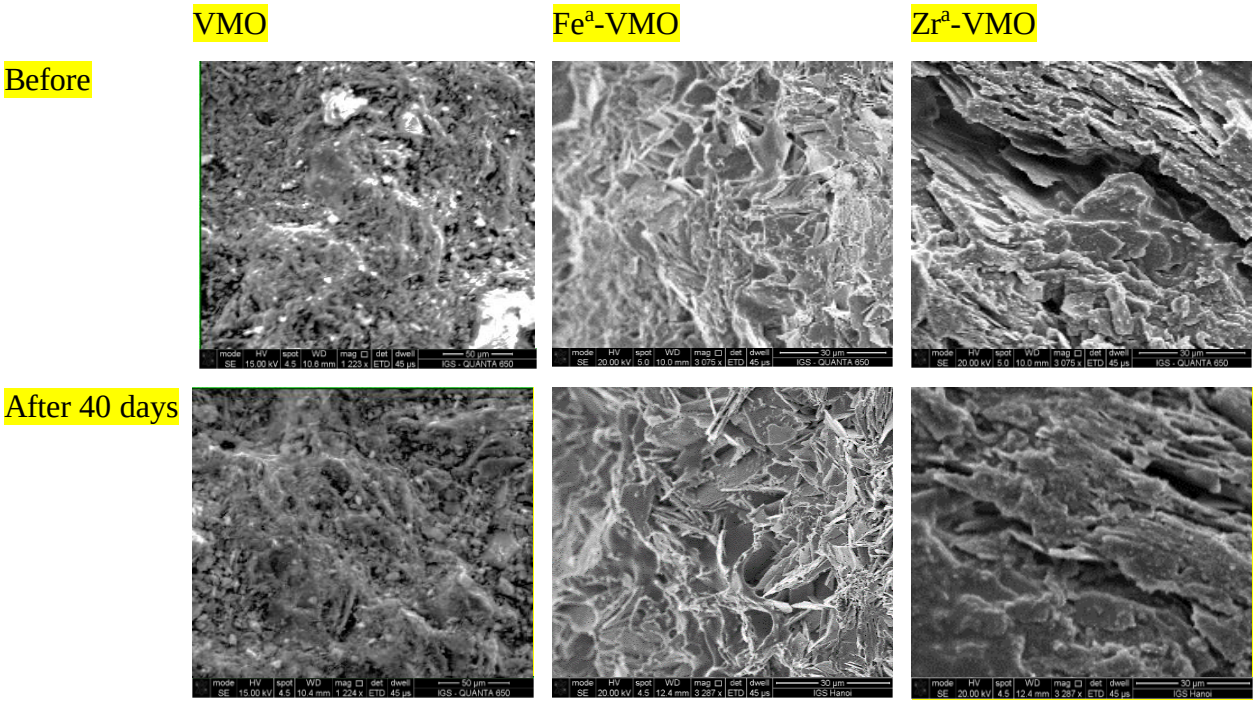

Fig. 1. SEM of adsorbents before and after 40 days of As(V) adsorption

3.2. Column studies

The column studies were carried out to evaluate the adsorption capacity of the adsorbents in dynamic conditions, and the effects of flow rate, and initial As(V) concentration on As breakthrough. Fig. 2 and 3 show the breakthrough curves of 9 columns belonging to original and modified VMOs at the flow rates of 0.15 and 0.5 L/h and influent As concentrations of 0.1 and 0.25 mg/L, respectively. The bed volumes (BV) at different times of breakthrough were calculated using the following formula where the flow rates 0.15 and 0.5 L/h correspond to 1.9 and 6.4 m/h, respectively [25]:

BV = flow rate (m/h) x time of breakthrough (h)/bed height (m) [4]

At any initial concentration and flow rate, the breakthrough curves of VMO were steeper than those of Fe[a]-VMO and Zr[a]-VMO (Fig. 2 and 3). It means that VMO saturated faster (at lower BV) than others did. Furthermore, the breakthrough curves of Zr[a]-VMO were steeper than those of Fe[a]-VMO. Consistent with the shapes of the breakthrough curves, the adsorption capacities of the three adsorbents followed the order, Fe[a]-VMO > Zr[a]-VMO > VMO (Table 3). This order is the same as that observed in the batch experiments for these three adsorbents [1].

The effect of the flow rate is depicted in Fig. 2. It can be seen that at the higher flow rate (0.5 L/h), the breakthrough curves were steeper, and the plateau of C_t/C_o for all adsorbent columns

occurred earlier (at lower BV) in comparison with those at the lower flow rate (0.15 L/h). Increase of flow rate causing steeper breakthrough curves and less time (BV) to reach C_t/C_o plateau has also been reported for adsorption of phosphate on ion exchange resin [18] and As adsorption on Fe grafted GAC [25] and magnetite/hematite/organic carbon composite [26]. These trends were explained as due to the larger amounts of As passing through the column per unit time at the higher velocity, resulting in a higher proportion of the available adsorption sites on the adsorbent getting saturated [18]. The results also showed that at both flow rates, the bed volume required for adsorbent saturation was higher for the adsorbent with greater adsorption capacity (Fe^a-VMO > Zr^a-VMO > VMO). The adsorption capacities of the modified adsorbents are many times higher than the adsorption capacity of the unmodified adsorbent, as found in our earlier batch study (Table 2).

The bed volumes of water containing As(V) (0.1 mg/L) treated by the three adsorbents to produce water with As(V) concentration below the WHO guideline concentration (C_{WHO} = 10 µg/L) are presented in Table 2. The results show that the bed volumes treated by Zr^a-VMO and Fe^a-VMO were 6 and 8 times higher than for VMO at the flow rate of 0.15 L/h, respectively. When the flow rate was increased to 0.5 L/h, the corresponding bed volumes for Zr^a-VMO and Fe^a-VMO were 12 and 16 times higher than for unmodified VMO, respectively. This means that much larger amounts of As contaminated water can be treated to produce water with safe levels of As by the modified VMOs rather than the unmodified VMO. Such larger amounts of treated water generated by the modified VMOs would lead to reduction of the cost of the treatment process per unit volume of water produced. This cost reduction is expected to cover the cost of Fe/Zr modification of VMO. The number of bed volumes treated is higher at the lower flow rate because the retention time of As in the column is longer, which allowed more effective interaction of As with the adsorbent leading to larger amounts of it being removed [25,26]. This is confirmed by the higher As adsorption capacity at the lower flow rate (Table 2). These results indicate that a higher volume of treated water can be produced by reducing the flow rate.

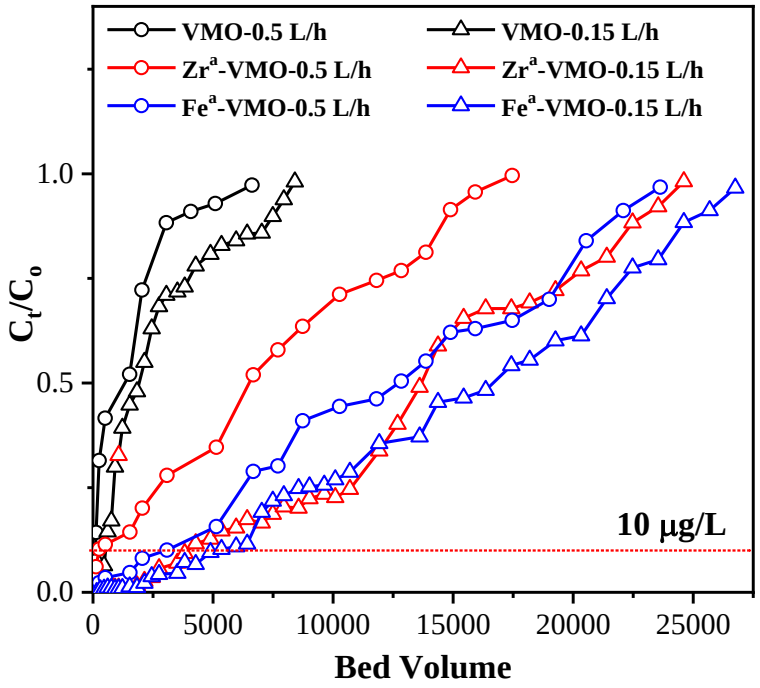

Fig. 2. The effect of flow rate on As(V) adsorption breakthrough in VMO, Fe^a-VMO, and Zr^a-VMO columns at an initial As(V) concentration of 0.1 mg/L. The 10 µg/L horizontal line within the figure indicates the WHO As concentration limit.

Table 2. The bed volumes of water treated by original and modified VMO to reduce As(V) concentration to WHO guideline concentration (10 µg/L) and the amount of As(V) adsorbed on adsorbents

Flow rate (L/h)	Adsorbent	Initial As(V) concentration (mg/L)	Bed volume	As(V) adsorption capacity (µg/g)
0.5	VMO	0.1	127	13
	Zr^a-VMO	0.1	1541	79
	Fe^a-VMO	0.1	2055	115
0.15	VMO	0.1	611	16
	Zr^a-VMO	0.1	3822	217
	Fe^a-VMO	0.1	4892	276
0.15	VMO	0.25	153	21
	Zr^a-VMO	0.25	2293	320
	Fe^a-VMO	0.25	2752	388

Fig. 3 shows the effect of the initial concentration of As(V) on As(V) removal at the same flow rate (0.15 L/h). The data showed that the columns operated with higher initial concentration (0.25 mg/L) would reach As saturation faster than those at a lower initial concentration (0.10 mg/L). Therefore, these columns treated fewer BV, and the breakthrough curves reached plateau faster than those at the lower concentration. This is because larger amounts of As enter the column at higher initial concentrations, and the adsorption sites are used up more quickly than when low As concentration enters the columns. Li et al. [26] also reported that an increase in the initial As concentration reduced the time taken for saturation of columns containing magnetite/hematite/organic carbon composite. However, when the initial concentration rose, although the number of bed volumes decreased, the As(V) adsorption capacity also increased (Table 2). This can be explained by the fact that at the higher initial concentration, more available adsorption sites were occupied by As rapidly [27].

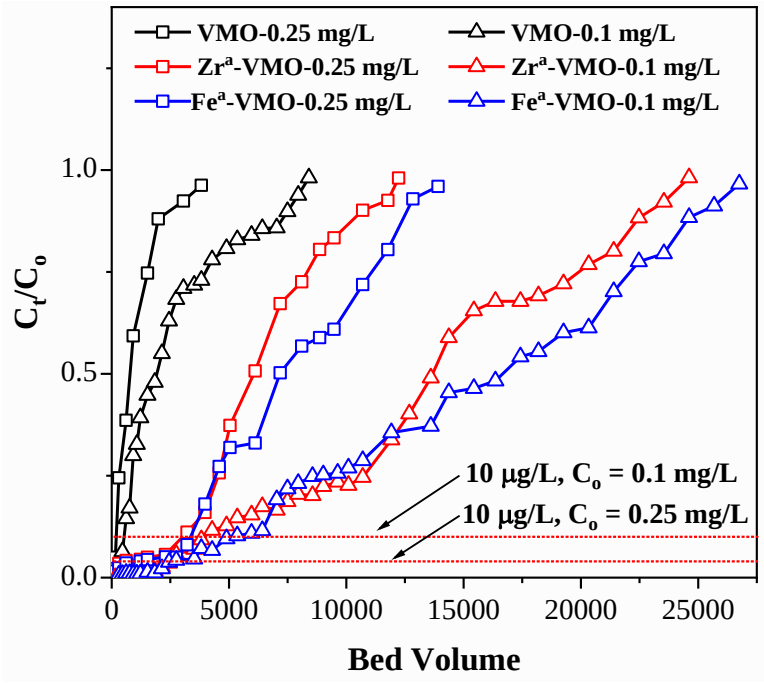

Fig. 3. The effect of As(V) initial concentration on As(V) removal by VMO, Fe^a-VMO, and Zr^a-VMO at the flow rate of 0.15 L/h. The 10 µg/L horizontal line within the figure indicates the WHO As concentration limit.

The Thomas model was used to describe the experimental data obtained in the column studies, on the effect of flow rate (Fig. 4) and the effect of initial concentration (Fig. 5). Table 3 presents the results of the model fits to data. At the same initial concentration (C_o), as the flow rate increased, the value of rate constant K_{Th} also increased, but the adsorption capacity q_T decreased. Conversely, at the same flow rate the value of q_{Th} increased, and K_{Th} decreased when the As(V) initial concentration increased. Therefore, a higher initial concentration, along with slower flow rate, would increase the As(V) adsorption capacity of adsorbent in the column study (Table 2) [27]. The reasons for these trends were explained in the previous section. The R^2 values were very high (> 0.92, that is > 92% of the variance in the data is explained by the model. The correlation coefficient r, which is the square root of R^2 is > 0.96 and this is very highly significant [28]), indicating that the experimental data fitted very well to the Thomas model, and this model can predict the adsorption performance very well under various experimental conditions. According to the prediction of the Thomas model, the maximum As(V) adsorption capacities of VMO, Zr^a-VMO, and Fe^a-VMO were 0.151, 0.925, and 1.145 mg/g, respectively, for C_o = 0.25 mg/L, and Q = 0.15 L/h (Table 3).

The adsorption capacities calculated from the breakthrough curves (q_{exp}) were only slightly lower than the respective Thomas adsorption capacities (Table 2), suggesting that the breakthrough

curves almost reached the plateau point (adsorbent saturation). The Thomas adsorption capacities for the modified adsorbents at the higher concentration and lower flow rate (Zr^a-VMO, and Fe^a-VMO with 0.925 and 1.145 mg/g, respectively) are much lower than the Langmuir maximum adsorption capacities (Zr^a-VMO, and Fe^a-VMO with 1.94 and 2.19 mg/g, respectively) determined in batch experiments [1]. The column adsorption capacities are lower than the batch adsorption capacities because in the batch experiments, adsorption reached equilibrium, and the Langmuir model predicted the maximum adsorption capacities at a higher solution As concentrations [25]. These conditions were different in the column experiment, where the adsorption capacities were measured at lower concentrations, and adsorption did not reach equilibrium. However, for the unmodified VMO, the adsorption capacities between the Thomas and Langmuir models calculated values were not very different, probably because of the very low adsorption capacity of VMO where maximum adsorption occurs at lower As concentrations.

The Thomas adsorption capacities obtained in this study were compared with those reported for other adsorbents in Table 4. The data shows that most adsorbents had adsorption capacity lower than VMO and its modified forms, except rice husk. However, the modified VMOs, Fe^a-VMO and Zr^a-VMO, had much higher adsorption capacities than all the other adsorbents.

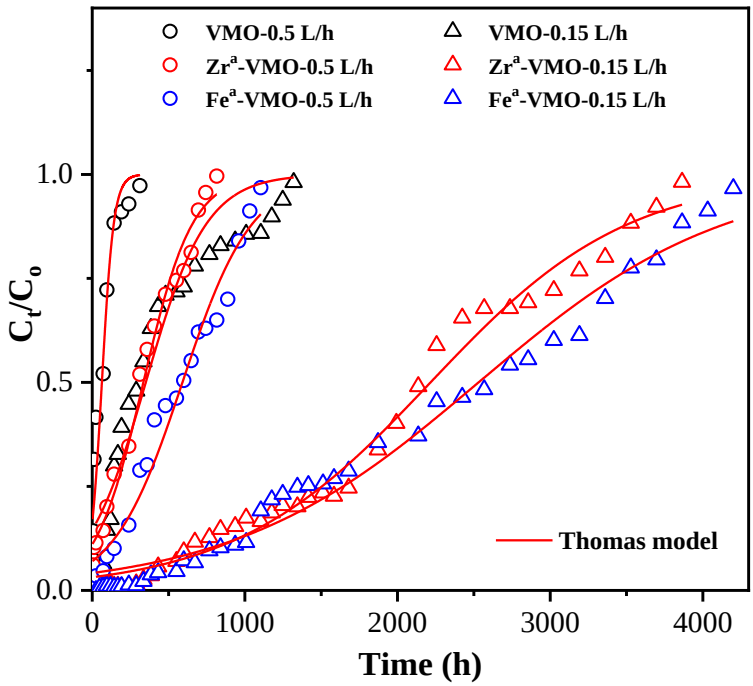

Fig. 4. Non-linear Thomas model fits to data on the removal of As(V) by VMO, Fe^a-VMO, and Zr^a-VMO at the two flow rates (C_o = 0.1 mg/L).

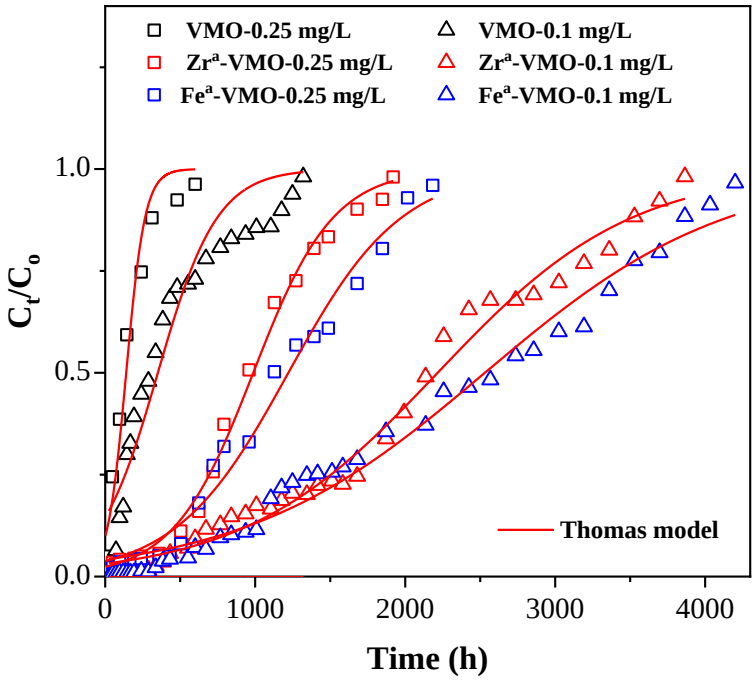

Fig. 5. Non-linear Thomas model fits to data on the removal of As(V) by VMO, Fe^a-VMO, and Zr^a-VMO at the two initial concentrations (Q = 0.15 L/h)

Table 3. Parameter values for the Thomas model fit to breakthrough data of columns loaded with VMO, Fe[a]-VMO, and Zr[a]-VMO.

Column	C_o = 0.1 mg/L Q = 0.15 L/h			C_o = 0.1 mg/L Q = 0.5 L/h			C_o = 0.25 mg/L Q = 0.15 L/h		
Adsorbent	VMO	Zr[a]-VMO	Fe[a]-VMO	VMO	Zr[a]-VMO	Fe[a]-VMO	VMO	Zr[a]-VMO	Fe[a]-VMO
q_{exp} (mg/g)	0.136	0.799	0.901	0.096	0.400	0.700	0.142	0.879	1.074
q_T (mg/g)	0.139	0.831	0.949	0.098	0.422	0.744	0.151	0.925	1.145
K_{Th} (L/h/mg)	0.043	0.015	0.012	0.258	0.062	0.044	0.037	0.015	0.011
R^2	0.92	0.98	0.98	0.94	0.98	0.97	0.96	0.99	0.98

Table 4. Comparison of Thomas adsorption capacities obtained in the current study with those reported in other studies

Adsorbent	As (V) concentration (mg/L)	Flow rate (L/h)	Thomas adsorption capacity (mg/g)	Reference
Multi walled carbon nanotubes	0.04	1.20	0.014	[29]
Rice husk	0.07	0.42	0.416	[30]
Natural pozzolan	0.40	0.24	0.003	[31]
Thioglycolated sugarcane carbon	1.50	0.18	0.083	[32]
VMO	0.25	0.15	0.151	This study
Zr[a]-VMO	0.25	0.15	0.925	This study
Fe[a]-VMO	0.25	0.15	1.145	This study

3.3. Cost estimation for treatment

The market price of VMO is A$0.40/kg. The costs of the modified VMOs are calculated using the industrial prices of the chemicals, $Fe(NO_3)_3{\cdot}9H_2O$ (A$0.40/kg), $ZrOCl_2.8H_2O$ (A$1.64/kg), and NaOH (A$0.30/kg), employed in the modification procedure (prices of the chemicals are obtained from https://www.alibaba.com/product-detail/ferric-nitrate; https://www.alibaba.com/product-detail/36-zirconium-oxychloride-ZrOCl2-8H2O; https://www.alibaba.com/product-detail/Bulk-price-for-industrial-1-kg) and the quantities of the chemicals used in the modification. The quantities of the chemicals used are obtained from Nguyen

et al. (2020). Based on this calculation the cost of Fe-VMO and Zr-VMO are estimated to be A$0.80/kg and A$1.67/kg, respectively.

The cost of treating 1 m^3 water containing 0.1 mg As(V)/L to produce safe drinking water (<10 µg As/L) was calculated by multiplying the cost of the adsorbent by the weight of adsorbent in the column (40 g) divided by the volume of water treated (m^3). The volumes of water treated by VMO, Zr-VMO, and Fe-VMO at the flow rate of 0.15 L/h are 0.0144 m^3, 0.0900 m^3, and 0.1152 m^3, respectively (time (h) taken to reach 10 µg As/L in treated water x flow rate (L/h)/1000 L/m^3). Based on this calculation the costs of treating 1 m^3 water by VMO, Zr-VMO, and Fe-VMO are estimated to be A$1.111, A$0.742, and A$0.278, respectively. The lower treatment costs of the modified VMOs compared to the unmodified VMO is due to the larger volumes of water treated, despite their higher costs. The treatment cost of Fe-VMO is lower than that of Zr-VMO because its production cost is lower, and it treated a higher volume of water. The cost calculated here applies only to a single use of the adsorbents, until they get exhausted to produce safe levels of As in the treated water. However, the exhausted adsorbents can be rejuvenated by desorbing the adsorbed As and repeatedly used. Repeated use of the adsorbents will considerably decrease the cost of the treatment.

3.4. Solidification/Stabilisation

3.4.1 Characteristic of concrete

3.4.1.1 SEM, EDS, XRD

The SEM images revealed that generally, the surface of the concrete mix samples was rough and heterogeneous, and there was no visible change in the surface morphology of the samples before and after incorporating the contaminated unmodified VMO and modified VMOs (Fig. 6a, b). The absence of any change in morphology could be because the VMO derived from the mines, contains many minerals/compounds whose morphologies are similar to the sand and aggregate gravels of the concrete mixture.

The EDS results showed that As element was not detected on the surface of all concrete samples (Fig. 6c). Only the elements included in the compositions of Portland cement, sand, and aggregate gravels were identified, which included Si, Ca, and Al [33,34]. The spectra of C5, C10, C15, and C20 were similar to that of C0, with no change in peak intensities, and no peak disappeared, or a new peak appeared after adding the adsorbent wastes into the concrete mixture.

Similarly, the XRD analysis of the various mixtures of concrete showed only peaks for the major minerals of concrete (Fig. 6d). The peaks at $2\theta = 21^{o}$, 26.5^{o}, 50^{o}, and 60^{o} are characteristics of quartz. The peak at $2\theta = 21^{o}$ can additionally be due to the presence of gismondine [35]. The

peaks around 2θ = 28 º - 29 º are due to calcite and feldspars [35]. No As(V) minerals were identified in the XRD result and this is consistent with the EDS finding, which did not show any As elemental peak. This may be because the amount of As(V) in the adsorbent waste (< 0.05%) and the percentage of waste in the concrete mixture (< 7%) were very small in comparison to the large amount of concrete mixture. However, Singh and Pant [15] detected a peak for calcium arsenite in XRD for a concrete mixture of As waste (As adsorbed to activated alumina). This was probably due to the much higher proportion of As in the mixture (approximately 75% waste in the mixture and 12.5% As in adsorbent) than what was used in the current study.

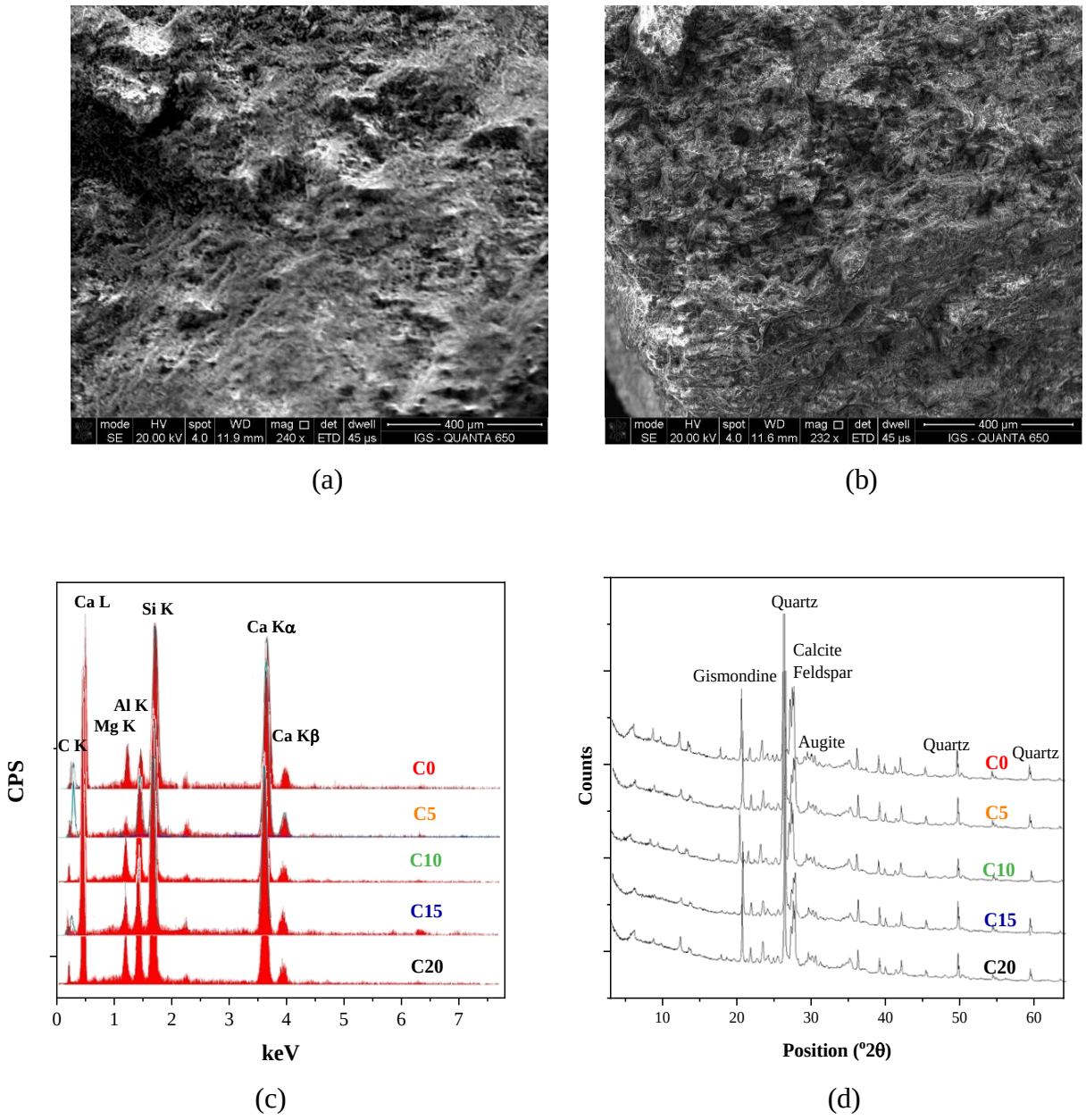

Fig. 6. SEM of the concrete mixture with (a) 0% and (b) 20% of adsorbent waste, (c) EDS spectrum, and (d) XRD patterns of five concrete mixture samples

3.4.1.2. Compressive strength, RCPT, and VPV

The compressive strength, RCPT, and VPV measurement results are presented in Table 5. The compressive strength results showed that after replacing sand by up to 20% exhausted unmodified and modified VMOs, the compressive strength declined only by a maximum of 4 MPa from the original value of 35 MPa. According to the Concrete Structures Standard of Australia AS 3600:2018, the concrete product with a minimum compressive strength of 20 - 32 MPa can be used to build footpaths and residential driveways (20 MPa), commercial and industrial floors not subject to vehicular traffic (25 MPa), and pavements or floors subject to pneumatic-tired traffic (32 MPa) [36]. Based on these standards, the concrete mixture produced by mixing exhausted adsorbent in this study can be used in many construction projects, such as the driveways, pavements, where humans will not have direct contact. The reason for the adsorbent waste addition not seriously affecting the compressive strength is that the original VMO adsorbent is also a crystalline inorganic material having similar mineral composition as sand and gravel in the concrete mixture, as well as due to the small amounts of waste added.

The ASTM C1202-19 determines the electrical conductance of concrete to provide a rapid indication of its resistance to the penetration of chloride ions via the rapid chloride penetrability test (RCPT) [34]. As the electrical charge passed through the concrete increases, the strength, performance, and the appearance of certain concrete structure will reduce, hence can lead to the corrosion of embedded steel bars within concrete [37]. Using this method, the charge passed through the five concrete mixes was measured to be 1175 - 1281 coulombs, which indicated that the chloride ion penetrability is low and the increase was only <1% with the adsorbant waste replacement of sand in all mixes (Table 5) [34]. The low charge transport through the concrete mixes suggests that the concrete mixes have greater compressive strength, denser materials with less porous microstructure, hence enhancing the chloride-ion transport resistance [34]. In contrast, Kaur et al. [34] found that when incinerated biomedical waste ash replaced sand in concrete at various proportions (5 - 20%), the charge increased from 1200 to 7825 coulombs. They stated that >10% replacement producing RCPT values of 6890 - 7825 coulombs was not acceptable as it can cause problems involving ions permeability.

According to standard ASTM C642-13, the VPV gives an indication of the amount of moisture and air, which can penetrate into the concrete. The VPV values of the 5 concrete mixes are in the 12.2 - 14.7% range (Table 5), which are similar to that of lightweight concrete having many applications [37]. As in the case of RCPT, VPV value also changed very little with an increase in percentage replacement of sand by the adsorbent waste in the concrete mix.

Table 5. The characteristics of the concrete mixes

Features	Unit	C0	C5	C10	C15	C20
Compressive strength	MPa	35.4	33.2	31.7	32.5	31.2
RCPT (charge passed)	coulombs	1270	1175	1225	1275	1281
VPV	%	12.2	13.5	14.4	12.6	14.7

3.4.2 Leaching test

VMO and modified VMOs have proved to be low-cost, safe, and environmentally friendly adsorbents [1]. The coating agents used to modify VMO to increase its As adsorption capacity, such as Fe and Zr, are also safe with regard to human health [17]. The commercial components (sand, cement, aggregates) used to make the concrete mixes have been employed widely and found to be very safe. Therefore, in investigating the potential toxicity of elements that might leach from the concrete mixes, only As was tested in the leachate.

The results of the leaching test are presented in Table 6. They indicate there is virtually no As leaching from the solidified/stabilised samples. Only in 3 samples (at pH 13 of C15, at pH 4 and 13 of C20) was As detected but its concentration is extremely low (0.0005, 0.0001 and 0.0014 mg/L, respectively). It is insignificant in comparison with the recommended limit stipulated in the toxicity characteristic leaching procedure (TCLP) of USEPA (up to 5 mg/L for As) [12]. The pH of all leachates in the leaching test, which had initial pH from 2 - 13, increased to 10-13 after the leaching test process. The highly alkaline conditions of the cement, due to the presence of $Ca(OH)_2$ would have increased the leachate pH and this could restrict the solubility of hazardous metals (Singh and Pant [15]. Both the high alkalinity and presence of a high concentration of Ca in cement would have resulted in the formation of calcium arsenic precipitates, and this may be the main mechanism that reduced or prevented the leachability of As [12,14].

Therefore, based on the results of compressive strength, RCPT, VPV, and As leachability tests, it can be concluded that the solidification/stabilisation product in this study is safe to dispose of or use as a structural construction material.

Table 6. As concentration in the leachates (mg/L)

Sample \ Initial pH	2	4	5.5	7	8	9	10.5	12	13
C0	0	0	0	0	0	0	0	0	0
C5	0	0	0	0	0	0	0	0	0
C10	0	0	0	0	0	0	0	0	0
C15	0	0	0	0	0	0	0	0	0.0005
C20	0	0.0001	0	0	0	0	0	0	0.0014

4. Conclusions

As(V) was effectively removed from water in columns packed with the original VMO and modified VMOs. The As(V) adsorption capacity and the number of bed volumes of contaminated water that can be treated to maintain the As(V) concentration below the WHO guideline concentration (C_{WHO} = 10 µg/L) increased in the order, VMO < Zr^a-VMO < Fe^a-VMO. An increase in the initial As concentration increased the adsorption capacity, but an increase in the flow rate of As solution through the column reduced the adsorption capacity of the adsorbent. The results indicated that higher volumes of treated water could be produced by reducing the flow rate. The Thomas model satisfactorily described the column breakthrough curves. The solidification/stabilisation method of disposing of the As waste in the exhausted adsorbents was applied successfully by encapsulating the exhausted adsorbents with concrete made from cement, sand and gravels. This solidified material had satisfactory compressive strength, RCPT, and VPV, which demonstrated good stability of the material, and therefore it can be used as a building material in construction work. The amount of As(V) leaching from these materials into the environment was found to be very negligible.

Acknowledgement

The project was supported by the Australian Government Department of Foreign Affairs and Trade's (DFAT) innovationXchange (iXc).

References

[1] T.T.Q. Nguyen, P. Loganathan, T.V. Nguyen, S. Vigneswaran, Removing arsenic from water with an original and modified natural manganese oxide ore: batch kinetic and equilibrium adsorption studies, Environ. Sci. Pollut. Res. (2020), 27(5), 5490-5502.

[2] M.K. Mondal, R. Garg, A comprehensive review on removal of arsenic using activated

carbon prepared from easily available waste materials, Environ. Sci. Pollut. Res. (2017), 24(15), 13295-13306.

[3] P. Loganathan, S. Vigneswaran, J. Kandasamy, N.S. Bolan, Removal and recovery of phosphate from water using sorption, Crit. Rev. Environ. Sci. Technol. (2014), 44(8), 847-907.

[4] D. Mohan, C.U. Pittman, Arsenic removal from water/wastewater using adsorbents-A critical review, J. Hazard. Mater. (2007), 142(1-2), 1-53.

[5] M.F. Ahmed, An Overview of Arsenic Removal Technologies in Bangladesh and India, Civ. Eng. (2001), pp 5-7.

[6] S. Chakravarty, V. Dureja, G. Bhattacharyya, S. Maity, S. Bhattacharjee, Removal of arsenic from groundwater using low cost ferruginous manganese ore, Water Res. (2002), 36(3), 625-632.

[7] M. Chiban, Application of low-cost adsorbents for arsenic removal: A review, J. Environ. Chem. Ecotoxicol. (2012), 4(5), 91-102.

[8] F. Kabir, S. Chowdhury, Arsenic removal methods for drinking water in the developing countries: technological developments and research needs, Environ. Sci. Pollut. Res. (2017), 24(31), 24102-24120.

[9] G.S. YF Li, D Wang, B Li, L Dong, Development of Arsenic Removal Technology from Drinking Water in Developing Countries, Arsen. Contam. Asia, Springer. (2019) 163–179.

[10] M. Leist, R.J. Casey, D. Caridi, The management of arsenic wastes: Problems and prospects, J. Hazard. Mater. (2000), 76(1), 125-138.

[11] T.V. Nguyen, P. Loganathan, S. Vigneswaran, S. Krupanidhi, T.T.N. Pham, H.H. Ngo, Arsenic waste from water treatment systems: Characteristics, treatments and its disposal, Water Sci. Technol. Water Supply. (2014), 14(6), 939-950.

[12] C. Jing, S. Liu, X. Meng, Arsenic leachability and speciation in cement immobilized water treatment sludge, Chemosphere. (2005), 59(9), 1241-1247. https://doi.org/10.1016/j.chemosphere.2004.11.039.

[13] I.H. Yoon, D.H. Moon, K.W. Kim, K.Y. Lee, J.H. Lee, M.G. Kim, Mechanism for the stabilization/solidification of arsenic-contaminated soils with Portland cement and cement kiln dust, J. Environ. Manage. (2010), 91(11), 2322-2328. https://doi.org/10.1016/j.jenvman.2010.06.018.

[14] C. Sullivan, M. Tyrer, C.R. Cheeseman, N.J.D. Graham, Disposal of water treatment wastes containing arsenic - A review, Sci. Total Environ. (2010), 408(8), 1770-1778. https://doi.org/10.1016/j.scitotenv.2010.01.010.

[15] T.S. Singh, K.K. Pant, Solidification/stabilization of arsenic containing solid wastes using

portland cement, fly ash and polymeric materials, J. Hazard. Mater. (2006), 131(1), 29-36. https://doi.org/10.1016/j.jhazmat.2005.06.046.

[16] J.D. Lincoln, O.A. Ogunseitan, A.A. Shapiro, J.D.M. Saphores, Leaching assessments of hazardous materials in cellular telephones, Environ. Sci. Technol. (2007), 41(7), 2572-2578. https://doi.org/10.1021/es0610479.

[17] T.T.Q. Nguyen, P. Loganathan, T.V. Nguyen, S. Vigneswaran, H.H. Ngo, Iron and zirconium modified luffa fibre as an effective bioadsorbent to remove arsenic from drinking water, Chemosphere. (2020), 127370. https://doi.org/10.1016/j.chemosphere.2020.127370.

[18] T. Nur, P. Loganathan, T.C. Nguyen, S. Vigneswaran, G. Singh, J. Kandasamy, Batch and column adsorption and desorption of fluoride using hydrous ferric oxide: Solution chemistry and modeling, Chem. Eng. J. (2014), 247, 93-102. https://doi.org/10.1016/j.cej.2014.03.009.

[19] H.H. Hammud, A. Shmait, N. Hourani, Removal of Malachite Green from water using hydrothermally carbonized pine needles, RSC Adv. (2015), 5, 7909-7920. https://doi.org/10.1039/c4ra15505j.

[20] D. Baweja, H. Roper, V. Sirivivatnanon, Improved electrochemical determinations of chloride-induced steel corrosion in concrete, ACI Mater. J. (2003), 100(3), 228-238. https://doi.org/10.14359/12624.

[21] A. El-Zohairy, H. Hammontree, E. Oh, P. Moler, Temperature Effect on the Compressive Behavior and Constitutive Model of Plain Hardened Concrete, Materials (Basel). (2020), 13(12), 2801. https://doi.org/10.3390/ma13122801.

[22] H.N. Xuan, L.T. Van, B.I. Bulgakov, O. V. Alexandrova, Strength, chloride resistance and corrosion reinforced of High-strength concrete, in: J. Phys. Conf. Ser. (2020), pp. 012193. https://doi.org/10.1088/1742-6596/1425/1/012193.

[23] E.E. Kumendong, S.W.M. Supit, H. Mantiri, Effects of Coconut Sawdust on Mechanical Properties and Porosity of Concrete Mixtures, J. Sustain. Eng. Proc. Ser. (2019), 1(2), 187-193. https://doi.org/10.35793/joseps.v1i2.26.

[24] D.S. Kosson, A.C. Garrabrants, R. DeLapp, H.A. van der Sloot, PH-dependent leaching of constituents of potential concern from concrete materials containing coal combustion fly ash, Chemosphere. (2014), 103, 140-147. https://doi.org/10.1016/j.chemosphere.2013.11.049.

[25] M. Kalaruban, P. Loganathan, T.V. Nguyen, T. Nur, M.A. Hasan Johir, T.H. Nguyen, M.V. Trinh, S. Vigneswaran, Iron-impregnated granular activated carbon for arsenic removal: Application to practical column filters, J. Environ. Manage. (2019), 239, 235-24.

https://doi.org/10.1016/j.jenvman.2019.03.053.

[26] Y. Li, Y. Zhu, Z. Zhu, X. Zhang, D. Wang, L. Xie, Fixed-bed column adsorption of arsenic(V) by porous composite of magnetite/hematite/carbon with eucalyptus wood microstructure, J. Environ. Eng. Landsc. Manag. (2018), 26(1), 38-56. https://doi.org/10.3846/16486897.2017.1346513.

[27] R. Han, Y. Wang, X. Zhao, Y. Wang, F. Xie, J. Cheng, M. Tang, Adsorption of methylene blue by phoenix tree leaf powder in a fixed-bed column: experiments and prediction of breakthrough curves, Desalination. (2009), 245, 284-297. https://doi.org/10.1016/j.desal.2008.07.013.

[28] D.A. Preece, T.M. Little, F.J. Hills, Agricultural Experimentation: Design and Analysis, Biometrics. (1982), 524-525. https://doi.org/10.2307/2530470.

[29] I. Ali, Microwave assisted economic synthesis of multi walled carbon nanotubes for arsenic species removal in water: Batch and column operations, J. Mol. Liq. (2018), 271, 677-685. https://doi.org/10.1016/j.molliq.2018.09.021.

[30] Z. Asif, Z. Chen, Removal of arsenic from drinking water using rice husk, Appl. Water Sci. (2017), *7*(3), 1449-1458. https://doi.org/10.1007/s13201-015-0323-x.

[31] G.P. Kofa, S. NdiKoungou, G.J. Kayem, R. Kamga, Adsorption of arsenic by natural pozzolan in a fixed bed: Determination of operating conditions and modeling, J. Water Process Eng. (2015), 6, 166-173. https://doi.org/10.1016/j.jwpe.2015.04.006.

[32] P. Roy, N.K. Mondal, S. Bhattacharya, B. Das, K. Das, Removal of arsenic(III) and arsenic(V) on chemically modified low-cost adsorbent: batch and column operations, Appl. Water Sci. (2013), 3(1), 293-309. https://doi.org/10.1007/s13201-013-0082-5.

[33] P.C. Aïtcin, Portland cement, in: Sci. Technol. Concr. Admixtures. (2016), pp. 27-51.

[34] H. Kaur, R. Siddique, A. Rajor, Influence of incinerated biomedical waste ash on the properties of concrete, Constr. Build. Mater. (2019), 226, 428-441. https://doi.org/10.1016/j.conbuildmat.2019.07.239.

[35] M. Karanac, M. Đolić, Đ. Veljović, V. Rajaković-Ognjanović, Z. Veličković, V. Pavićević, A. Marinković, The removal of Zn2+, Pb2+, and As(V) ions by lime activated fly ash and valorization of the exhausted adsorbent, Waste Manag. (2018), 78, 366-378. https://doi.org/10.1016/j.wasman.2018.05.052.

[36] M.K. Khalajestani, A. Parvez, S.J. Foster, H. Valipour, G. McGregor, Strength and ductility of high-strength concrete columns reinforced with high-strength steel, in: FIB 2018 - Proc. 2018 Fib Congr. Better, Smarter, Stronger. (2019).

[37] A. Sekar, G. Kandasamy, Study on durability properties of coconut shell concrete with coconut fiber, Buildings. (2019), 9(5), 107. https://doi.org/10.3390/buildings9050107.